Aminobisphosphonates Synergize with Human Cytomegalovirus To Activate the Antiviral Activity of Vγ9Vδ2 Cells

Charline Daguzan, Morgane Moulin, Hanna Kulyk Barbier, Christian Davrinche, Suzanne Peyrottes, Eric Champagne

The Journal of Immunology

Aminobisphosphonates Synergize with Human Cytomegalovirus To Activate the Antiviral Activity of Vγ9Vδ2 Cells

Charline Daguzan, Morgane Moulin, Hanna Kulyk-Barbier, Christian Davrinche, Suzanne Peyrottes and Eric Champagne

J Immunol 2016; 196:2219-2229; Prepublished online 27 January 2016;
doi: 10.4049/jimmunol.1501661
http://www.jimmunol.org/content/196/5/2219

The Journal of Immunology is published twice each month by
The American Association of Immunologists, Inc.,
1451 Rockville Pike, Suite 650, Rockville, MD 20852

Print ISSN: 0022-1767 Online ISSN: 1550-6606.

Aminobisphosphonates Synergize with Human Cytomegalovirus To Activate the Antiviral Activity of Vγ9Vδ2 Cells

Charline Daguzan,*,†,‡,§ Morgane Moulin,*,†,‡,§ Hanna Kulyk-Barbier,¶ Christian Davrinche,*,†,‡,§ Suzanne Peyrottes,‖ and Eric Champagne*,†,‡,§

Human Vγ9Vδ2 T cells are activated through their TCR by neighboring cells producing phosphoantigens. Zoledronate (ZOL) treatment induces intracellular accumulation of the phosphoantigens isopentenyl pyrophosphate and ApppI. Few attempts have been made to use immunomanipulation of Vγ9Vδ2 lymphocytes in chronic viral infections. Although Vγ9Vδ2 T cells seem to ignore human CMV (HCMV)–infected cells, we examined whether they can sense HCMV when a TCR stimulus is provided with ZOL. Fibroblasts treated with ZOL activate Vγ9Vδ2 T cells to produce IFN-γ but not TNF. Following the same treatment, HCMV-infected fibroblasts stimulate TNF secretion and an increased production of IFN-γ, indicating that Vγ9Vδ2 cells can sense HCMV infection. Increased lymphokine production was observed with most clinical isolates and laboratory HCMV strains, HCMV-permissive astrocytoma, or dendritic cells, as well as "naive" and activated Vγ9Vδ2 cells. Quantification of intracellular isopentenyl pyrophosphate/ApppI following ZOL treatment showed that HCMV infection boosts their accumulation. This was explained by an increased capture of ZOL and by upregulation of HMG-CoA synthase and reductase transcription. Using an experimental setting where infected fibroblasts were cocultured with γδ cells in submicromolar concentrations of ZOL, we show that Vγ9Vδ2 cells suppressed substantially the release of infectious particles while preserving uninfected cells. Vγ9Vδ2 cytotoxicity was decreased by HCMV infection of targets whereas anti–IFN-γ and anti-TNF Abs significantly blocked the antiviral effect. Our experiments indicate that cytokines produced by Vγ9Vδ2 T cells have an antiviral potential in HCMV infection. This should lead to in vivo studies to explore the possible antiviral effect of immunostimulation with ZOL in this context. *The Journal of Immunology*, **2016, 196: 2219–2229.**

In humans, γδ T cells represent 1–5% of peripheral T cells and are subdivided in subsets expressing preferential combinations of variable γ and variable δ TCR regions. The largest subset in humans expresses a TCR with variable γ9 and δ2 regions (GV2S1/DV102S1 according to the official World Health Organization nomenclature; hereafter referred to as Vγ9Vδ2 cells), is absent in rodents, and expands in vivo or in vitro after contacting cells producing or loaded with small phosphorylated compounds called phosphoantigens. Exogenous phosphoantigens are produced by several bacteria and parasites, and thus Vγ9Vδ2 cells are components of the innate defense against these pathogens (1). Endogenous phosphoantigens such as isopentenyl pyrophosphate (IPP) are also ubiquitously produced by eukaryotic cells as intermediates of the mevalonate pathway (2). IPP accumulation occurs naturally in some tumors following perturbation of this pathway but it can also be induced by aminobisphosphonate (ABP) drugs. ABPs limit bone resorption and this property is widely used in the clinic for treatment of demineralizing diseases such as osteoporosis, rheumatoid arthritis, Paget disease, and cancer metastases. More recently it has been demonstrated that they block the mevalonate pathway enzyme farnesyl pyrophosphate synthase and subsequently promote intracellular IPP accumulation in target cells (3). This promotes the recognition and killing of tumors by Vγ9Vδ2 cells (3, 4) and this property is exploited in anticancer immunotherapeutic approaches using ABPs (5). Multiple clinical trials have been performed to evaluate the beneficial effect of Vγ9Vδ2 T cell stimulation by ABPs in conjunction with IL-2 administration and encouraging results have been obtained, showing the relative safety and adjuvant potential of this approach for antitumor therapy (5) and for restoring immune competence in HIV patients (6).

The Vγ9Vδ2 T cell response to APB-induced phosphoantigen accumulation is TCR- and CD277 (butyrophilin BTN3A1)-dependent (7–9). Intracellular phosphoantigens can bind to the cytoplasmic domain of BTN3A1, and this interaction is sensed by the Vγ9Vδ2 TCR in a manner that is still incompletely understood but may involve a conformational rearrangement of BTN3 and other protein complexes such as periplakin and F1-ATPase, conferring the cells an increased sensitivity to Vγ9Vδ2 killing activity (10–14).

Non-Vδ2 γδ T cells expand in response to acute HCMV infections in immunocompromised patients or following placental infections, where they are thought to provide some protection in

*Centre de Physiopathologie de Toulouse Purpan, 31024 Toulouse, France; †INSERM, U1043, 31024 Toulouse, France; ‡CNRS, UMR5282, 31024 Toulouse, France; §Université Toulouse III Paul-Sabatier, 31062 Toulouse, France; ¶Laboratoire d'Ingénierie des Systèmes Biologiques et des Procédés, Institut National des Sciences Appliquées, Plateforme MetaToul, UMR Institut National des Sciences Appliquées/CNRS 5504–UMR INSA/Institut National de la Recherche Agronomique 792, 31400 Toulouse, France; and ‖Institut des Biomolécules Max Mousseron, UMR 5247 CNRS-Université Montpellier 2-Ecole Nationale Supérieure de Chimie de Montpellier, 34095 Montpellier, France

Received for publication July 28, 2015. Accepted for publication December 18, 2015.

This work was supported by Fondation pour la Recherche Médicale Grant DCM20121225761.

Address correspondence and reprint requests to Dr. Eric Champagne, Centre de Physiopathologie de Toulouse Purpan, Centre Hospitalier Universitaire Purpan, BP 3028, 31024 Toulouse Cedex 03, France. E-mail address: eric.champagne@inserm.fr

The online version of this article contains supplemental material.

Abbreviations used in this article: ABP, aminobisphosphonate; ApppI, triphosphoric acid 1-adenosin-5′-yl ester 3-(3-methylbut-3-enyl) ester; CM, complete medium; DC, dendritic cell; HCMV, human CMV; IPP, isopentenyl pyrophosphate; LOD, limit of detection; LOQ, limit of quantification; MOI, multiplicity of infection; MRM, multiple reaction monitoring; ZOL, zoledronate.

conjunction with CD8 and NK cells (15). Although alterations of the Vγ9Vδ2 subset are observed in multiple viral contexts such as HIV or hepatitis C virus infections (16–19), the role of these cells is not clear. Human Vγ9Vδ2 cells that have been activated in vivo with ABPs can control influenza virus–mediated disease after transfer in RAG-deficient mice (20). Thus, Vγ9Vδ2 cells, as well as non-Vδ2 subsets, could possibly exert antiviral activity either naturally or following specific immunostimulation.

HCMV is a β-herpesvirus that replicates in epithelial and endothelial cells, fibroblasts, and other cell types following primary infection, and it persists life-long in a latent state in myeloid lineage cells, which constitute a reservoir for subsequent reactivation, with deleterious consequences in immunocompromised individuals. There is at present no possibility to clear HCMV infection. HCMV persistence is largely influenced by viral factors that interfere with apoptosis and with the MHC class I peptide Ag presentation pathway, allowing the escape of infected cells from CD8 T cells (21). Additionally, several viral microRNAs and proteins downmodulate the expression of stress molecules on the surface of HCMV-infected cells. This is the case for UL16-binding proteins and MHC class I chain–related Ags, which stimulate activating receptors on NK cells and γδ cells (22, 23).

The present study was undertaken to examine in vitro the immunotherapeutic potential of Vγ9Vδ2 immunomanipulation in the context of HCMV infection because pharmacological stimulation of these cells is more readily achievable than that of non-Vδ2 cells. How Vγ9Vδ2 cells behave when they are challenged with HCMV-infected cells and the effect of Vγ9Vδ2-specific immune manipulation have not been reported. Although Vγ9Vδ2 cells do not normally recognize HCMV-infected targets, we show in the present study that viral infection provides a potent additional stimulus when stimulating cells are concomitantly treated with ABPs. Consequently, doses of ABP that do not promote full activation of Vγ9Vδ2 cells by uninfected targets allow their activation by infected cells and subsequent inhibition/limitation of viral replication.

Materials and Methods

Cells and culture medium

Unless otherwise indicated, cultures were performed in complete medium (CM) containing RPMI 1640–GlutaMAX, sodium pyruvate, penicillin, streptomycin, and 10% heat-inactivated FCS (all reagents from Life Technologies).

Healthy donor PBMCs were purified by density gradient centrifugation over a Ficoll solution (Pancoll, PAN-Biotech) from buffy coats obtained from the Etablissement Français du Sang. MRC-5 (human embryonic lung fibroblasts, from Seromed) and U-373MG (human astrocytoma, from American Type Culture Collection) were maintained and infected with HCMV in DMEM-GlutaMAX medium (Life Technologies) supplemented with 10% heat-inactivated FCS, sodium pyruvate, and antibiotics.

Monocyte-derived dendritic cells (DCs) were generated as described previously (24). In brief, $CD14^+$ cells were purified from PBMCs by positive magnetic sorting (Miltenyi Biotec kit) and put to differentiate in CM containing IL-4 and GM-CSF (Miltenyi Biotec, 50 and 20 ng/ml, respectively) for 5 d.

For production of short-term Vγ9Vδ2 T cell lines, PBMCs were isolated from healthy donor buffy coat samples (obtained from the Etablissement Français du Sang). γδ T cells were purified by magnetic sorting with anti-TCRγ/δ microbeads (Miltenyi Biotec), and Vγ9Vδ2 cells (1×10^6) were expanded with (*E*)-4-hydroxy-3-methyl-but-2-enyl pyrophosphate phosphoantigen (Tebu-Bio; 10 nM) and IL-2 (400 IU/ml, after 48 h) in the presence of irradiated autologous PBMCs (30 Gy; 15×10^6 cells) and a mix of allogeneic lymphoblastoid cells (50 Gy, 1.5×10^6 cells) in CM, in a final volume of 10 ml. The cell concentration was kept close to 10^6 cells/ml by adding fresh medium and IL-2 every 2–3 d. After 19–22 d of culture, the percentage of Vγ9Vδ2 T cells was checked (usually >99% $V\gamma9^+$). When necessary, non-γδ cells were eliminated by negative magnetic sorting (Miltenyi Biotec) and cells were frozen.

The HCMV-responsive, Vδ2-negative γδ cell line (ND2LES) and the $CD8^+$ clone CMV-NLV (anti-HCMVpp65, HLA-A2 restricted) were provided by V. Pitard (Composantes Innées de la Réponse Immunitaire et de la Différenciation, Bordeaux, France) and S. Müller-Valitutti (Centre de Physiopathologie de Toulouse Purpan, Toulouse, France) respectively.

Virus strains, virus titration, inactivation, and infections

HCMV-AD169 was from the American Type Culture Collection. The endothelial cell-adapted strains VHL/E and TB40/E GFP were provided by C. Sinzger (Institute of Medical Virology, University of Tübingen, Tübingen, Germany) and M. Messerle (Department of Virology, Hannover Medical School, Hannover, Germany) respectively. Clinical isolates CON and TRI were provided by F. Halary (INSERM, UMR 1064, Nantes, France). All strains were amplified once on MRC-5 fibroblasts and collected from supernatants by ultracentrifugation at $70{,}000 \times g$ for 40 min and frozen in aliquots. Virus titers (fluorescence focus forming units/ml) of viral stocks and culture supernatants were determined after infection of MRC-5 cells with serial dilutions, followed by immunostaining of fibroblast layers at day 2 with anti–CMV-IE Ab and determination of fluorescence focus forming unit counts by immunofluorescence microscopy.

Viral inactivation by UV irradiation was performed by putting the virus suspension in an Eppendorf tube 3 cm below a Spectroline UV light (0.17 amp) for 20 min. For heat inactivation the viral suspension was put at 65°C for 30 min in a dry heating block.

HCMV infection of cell lines and fibroblasts was performed by adding virus dilutions to subconfluent (~80%) monolayers of cells, after having determined cell density to adjust for the desired multiplicity of infection (MOI). Cells were washed after 3 h. For the infection of DCs, the virus (VHL/E) was added to the cell suspension in culture wells (10^6 cells/ml) at an MOI of 5.

Detection of HCMV proteins by immunofluorescence microscopy

Cell monolayers in microtiter plates were washed with PBS, fixed with formaldehyde (4% in PBS [pH 7.3]) for 15 min at room temperature and permeabilized for 15 min in PBS containing 10 mM HEPES (pH 7.3), 3% bovine albumin, and 0.1% Triton X-100. Cells were stained with anti–HCMV-IE1/2 (anti-IEA; Biomérieux, Marcy-l'Étoile, France) or anti-pp28 (5C3, Abcam) followed by FITC-coupled anti-IgG $F(ab')_2$ Ab (Beckman Coulter), both steps at room temperature for 2 h. Nuclei were then stained with DAPI (1 μg/ml), and fluorescence images were acquired using a Zeiss Apotome microscope (wide field mode). For the quantitative evaluation of viral replication, images corresponding to nuclei staining for HCMV proteins (green channel) and total nuclei (DAPI, blue channel) were analyzed with ImageJ software and the automatic counting function. Two fields (~600 nuclei/field) were acquired for each well with the ×10 objective and counts were averaged.

Quantitative RT-PCR for HCMV-IE, HMG-CoA reductase and synthase

Cells were harvested and total RNA was isolated using the GenElute mammalian total RNA kit (Sigma-Aldrich). Reverse transcription was performed on 0.5 μg (IE) or 1 μg (HMG-CoA reductase and synthase) of total RNA (SuperScript III, Life Technologies), and real-time quantitative PCR was performed using the SYBR Green I Master system and LightCycler 480 (Roche). GAPDH was used as the endogenous control. The following primers were used: GAPDH, forward, 5′-TCATTTCCTGGTATGACAACG-3′, reverse, 5′-TCTTACTCCTTGGAGGCCAT-3′; HCMV-IE, forward, 5′-AACATAGTCTGCAGGAACGTC-3′, reverse, 5′-CCAAGAGAAAGATGGACCCTG-3′; HMG-CoA reductase, forward, 5′-GACCTTTCCAGAGCAAGCAC-3′, reverse, 5′-GCATCGAGGGTAAACGTAGG-3′; HMG-CoA synthase, forward, 5′-GGTTCCCTTGCATCTGTTCT-3′, reverse, 5′-TCCCTGCTAATTGCTGAGGT-3′.

The efficiency of amplification with all primer pairs was >0.98, and the specificity of amplification products was checked by denaturation curve analysis.

^{51}Cr-release assay

Adherent fibroblasts were labeled in flat-bottom microtiter wells (7500 cells/well) with 1 μCi ^{51}Cr-sodium chromate (PerkinElmer) in 40 μl CM for 1 h and washed three times with 150 μl RPMI 1640 medium. Vγ9Vδ2 effector T cells were added (100 μl) at the indicated E:T ratio, spun briefly to pellet cells, and incubated 4 h at 37°C. Cell-free supernatants (70 μl) were transferred to LumaPlates (Perkin-Elmer) and counted using a TopCount (PerkinElmer) counter. Spontaneous and maximum release values

were determined for each target with a specific treatment (infection and/or zoledronate [ZOL]), and were averaged from triplicates. Spontaneous release (spont) was determined from wells containing target cells only; maximum release (max) was obtained by replacing effector cells by 100 μl 1% Triton X-100. The percentage of specific lysis (%SL) was calculated as follows: $\%SL = 100 \times [(cpm_{sample} - cpm_{spont})/(cpm_{max} - cpm_{spont})]$.

Measure of cytokine expression

Release of IFN-γ and TNF in supernatants was measured by a standard ELISA (BD Biosciences kit) 48 h after addition of Vγ9Vδ2 T cells in cocultures with adherent cells in 96-well microtiter plates. In experiments with fresh PBMCs, cytokine expression was measured by FACS: adherent MRC-5 fibroblasts (2×10^5cells) were cultured, infected, and treated with ZOL in 24-well plates. Total PBMCs (10^6 cells/well) were added for 16 h in CM, and brefeldin A (5 μg/ml) was added during the last 4 h of coculture. Nonadherent lymphocytes were then harvested, washed, and surface stained with anti–Vγ9-PC5 mAbs (Beckman Coulter), then fixed and permeabilized with the Cytofix/Cytoperm kit (BD Biosciences) and stained with anti–IFN-γ-FITC and TNF-PE (BD Biosciences). After washing, fluorescence was acquired on an LSR II cytofluorometer (BD Biosciences) and analyzed with FlowJo software (Tree Star).

Cocultures with γδ T cells

Short-term cocultures of Vγ9Vδ2 T cell lines with adherent targets were performed at a 1:1 and 5:1 ratio for cytokine and cytotoxicity measurements, respectively. In these experiments, adherent targets were plated in 96-well microtiter plates and infected for the indicated times. When present, mevastatin, pamidronate (Sigma-Aldrich), and ZOL (Novartis) were added after infection at the indicated time and concentration before coculture and were washed out before the addition of T cells.

A different setting was used for prolonged 6-d cocultures of Vγ9Vδ2 cells with infected adherent cells to evaluate the level of viral replication. ZOL was added (0.05–0.4 μM) to adherent cells 24 h before infection to the culture medium in the T cell suspension and with fresh medium replacement at day 3 of the coculture to maintain the same final concentration. Microplates were used for immunofluorescence analysis (15×10^3 fibroblasts/well); for quantitative RT-PCR analysis of viral RNA and for the titration of live virus in supernatants, parallel cocultures were performed in 24-well plates (2×10^5 fibroblasts/well), with an identical E:T ratio of 0.2:1 and an MOI of ~0.2.

The role of IFN-γ and TNF in cocultures was assessed by adding anti–IFN-γ (B27, IgG1), anti-TNF (Mab1, IgG1) Abs, and IgG1 control Abs in the culture medium (10 μg/ml) at the start of the coculture and at day 3 with medium change. All Abs (BD Pharmingen) were azide free and endotoxin low.

Quantification IPP and triphosphoric acid 1-adenosin-5′-yl ester 3-(3-methylbut-3-enyl) ester by ion chromatography–coupled tandem mass spectrometry

MRC-5 fibroblasts were cultured in six-well plates to 80% confluence (10^6 cells in 2 ml CM) and infected with HCMV-AD169 (MOI of 1) for 48 or 96 h. ZOL and mevastatin were added at the indicated concentration during the last 16 and 40 h of culture, respectively. At the end of the culture, the fibroblast layer was washed twice with cold PBS and the plates were put on liquid nitrogen for fast freezing. The plate was then taken out and 5 ml cold lysis solution (acetonitrile/methanol/water, 4:4:2) and 180 μl isotope dilution mass spectrometry (IDMS) standard were added to ensure accurate quantification. Lysates were harvested in 15-ml polypropylene tubes by scrapping, vortexed extensively, and insoluble material was removed by quick centrifugation. Samples were evaporated under vacuum in a SC110A SpeedVac Plus (Thermo Fisher Scientific, Sunnyvale, CA) for 6 h and then stored at −80°C for further use. Dried samples were resolubilized in 100 μl milliQ water and IPP and triphosphoric acid 1-adenosin-5′-yl ester 3-(3-methylbut-3-enyl) ester (ApppI) were analyzed and quantified by ion chromatography coupled with a triple quadrupole mass spectrometer (ion chromatography–coupled tandem mass spectrometry) using the isotope dilution mass spectrometry method (25).

Liquid anion exchange chromatography was performed with the Thermo Scientific Dionex ICS-5000+ Reagent-Free HPIC system (Thermo Fisher Scientific) equipped with an eluent generator system (ICS-5000 EG, Dionex) for automatic base generation (KOH). Analytes were separated within 45 min, using a linear KOH gradient elution applied to an IonPac AS11 column (250 × 2 mm, Dionex) equipped with an AG11 precolumn (50 × 2 mm, Dionex) at a flow rate of 0.35 ml/min. The gradient was as follows: equilibration with 0.5 mM KOH, 1.1 min; KOH ramp from 0.5 to 4.1 mM, 1–9.5 min; constant concentration 5.1 min; isocratic ramp to 9.65 mM in 9.4 min; isocratic ramp to 60 mM in 8 min; isocratic ramp to 90 mM in 0.1 min; constant concentration 6.9 min; drop to 0.5 mM in 0.1 min; and equilibration at 0.5 mM KOH for 1.9 min. The column and autosampler temperatures were thermostated at 29°C and 4°C, respectively. The injected sample volume was 15 μl. Measures were performed in triplicates from separate cultures.

Tandem mass analyses were carried out in the negative mode with a 4000 QTRAP hybrid triple quadrupole/linear ion trap mass spectrometer (AB Sciex, Foster City, CA) equipped with a Turbo V source (AB Sciex/MDS Sciex, Toronto, ON, Canada) for electrospray ionization. The multiple reaction monitoring (MRM) approach was used for quantification of IPP and ApppI and was done by collision-activated dissociation using nitrogen as the collision gas at medium pressure. The nebulizer gas pressure was 50 psi, the desolvation gas pressure was 60 psi, the temperature was 55°C, and the capillary voltage was 4.2 kV. Instrument control, data acquisition, and data analysis were performed with Analyst version 1.5.2 software.

The MRM transitions used for quantification of the IPP and ApppI were 245.0→79.0 and 574.1→79.0, respectively. For absolute quantification of IPP and ApppI, the IPP U-^{13}C MRM transition was taken.

To determine the method's linearity, the limit of detection (LOD) and of quantification (LOQ), mixtures of the standard compounds at various concentrations (0.005–5 μmol/l) were analyzed. A linear range was observed between 0.01 and 5 μmol/l for both IPP and ApppI. For further quantification, linear ranges were chosen between 0.1 and 2.5 μmol/l and 0.01 and 0.3 μmol/l for IPP and ApppI, respectively. The variation of the ratio peak area ^{12}C/U-^{13}C with the concentration of ^{12}C standard was given by the linear regression equations $y = 93.747x - 4.3075$ (μmol/l), $R = 0.9992$ ($n = 5$) for IPP and $y = 248.06x + 0.6977$ (μmol/l), $R = 0.9995$ ($n = 5$) for ApppI, where R is the correlation coefficient and n is the number of points. The LOD and LOQ for IPP and ApppI were 0.1 and 0.3 μmol/l (IPP) and 0.01 and 0.03 μmol/l (ApppI), respectively, calculated by using the calibration curve method with the following equations: $LOD = 3Sy/x \div b$ and $LOQ = 10\ Sy/x \div b$, were b is the intercept of regression line and Sy/x is the SD of the intercept.

Capture of FluorZol

FluorZol (26) was provided by D. Kabelitz (Department of Immunology, Kiel University, Kiel, Germany). MRC-5 fibroblasts were cultured in 24-well plates to 80% confluence (1.5×10^5 cells, 0.5 ml/well), infected with HCMV-AD169, and pulsed with FluorZol as indicated. At the end of the culture, fibroblasts were trypsinized, washed twice, and fixed with 2% paraformaldehyde for 15 min. Fluorescence was acquired on an LSR II cytofluorometer (BD Biosciences) and analyzed with FlowJo software (Tree Star).

Statistical analyses

Most analyses were performed with Prism version 5 software (GraphPad Software). A nonparametric Wilcoxon test was used for all single point comparisons. Dose-response curves were compared by covariance analyses (ANCOVA, ExcelStat software) after linearization of data by log or logit transformation of variables. The slopes of linear regression lines were compared, and a p value <0.05 was considered significant.

Results

Lymphokine secretion by Vγ9Vδ2 cell lines

We wanted to know whether Vγ9Vδ2 T cells could detect signs of infection by HCMV. To this end we challenged short-term Vγ9Vδ2 cell lines (>95% Vγ9$^+$) with MRC-5 fibroblasts that were infected or not with the HCMV-AD169 laboratory strain and we measured IFN-γ and TNF secretion, the main cytokines produced by Vγ9Vδ2 cells. In the absence of additional stimulus, no significant lymphokine secretion was detected. Then we tested whether infection could be sensed by Vγ9Vδ2 T cells after treatment of fibroblasts with ABPs to promote intracellular production of phosphoantigens and provide a specific stimulation of the Vγ9Vδ2 TCR. To this end, HCMV-infected and control uninfected fibroblasts were treated 16 h with various doses of ZOL. When Vγ9Vδ2 cells were stimulated with ZOL-treated uninfected fibroblasts, increasing amounts of IFN-γ were released in response to increasing doses of ZOL, whereas TNF secretion was barely detectable. When Vγ9Vδ2 cells were challenged with infected ZOL-treated cells, large and dose-dependent amounts of TNF

were released and IFN-γ production was increased. The effect of viral infection on IFN-γ and TNF release was abrogated by virus inactivation by UV or heat treatment (65°C, 30 min) (27) and was thus dependent on viral transcription and/or replication (Fig. 1A).

The stimulatory activity of ABP-treated fibroblasts increased with the length of infection, from 24 to 96 h (Fig. 1B, 1C). Longer infection times were not tested because virus cycle completion induced significant fibroblast lysis. HCMV infection of fibroblasts also increased the IFN-γ response of Vγ9Vδ2 T cells when another ABP, pamidronate, was used instead of ZOL (Fig. 1C). No significant IFN-γ and no TNF were detected in control fibroblast cultures without γδ cells, treated or not with ABPs, infected or not (Fig. 1C and data not shown).

A Vδ2-negative γδ cell line (ND2LES) and a CD8 clone (CMV-NVL) reactive against HCMV were also tested. Although both cell lines increased their secretion of IFN-γ in response to HCMV-infected cells, this was not affected by the treatment of fibroblasts with ZOL (Fig. 1D). TNF was never detected in these conditions (not shown). Thus, viral replication in AD169-infected fibroblasts synergizes with ABP treatment for the stimulation of IFN-γ and TNF secretion by Vγ9Vδ2 cells specifically.

Influence of the HCMV strain and of the host cell type

The AD169 HCMV strain is a laboratory-adapted isolate and carries multiple genomic deletions that alter tropism and virus–host interactions (28). To determine whether other strains of HCMV could similarly boost lymphokine secretion by Vγ9Vδ2 T cells, we tested the laboratory strains VHL/E and TB40/E and two low-passage clinical isolates (CON, TRI). TB40/E did not significantly increase cytokine production whereas infection with other strains led to increased production of IFN-γ and TNF, although their efficiency to promote TNF release was variable. Differences between strains for the speed of viral cycle progression are not excluded. Thus, the Vγ9Vδ2 cell response is dependent on the virus, but most tested HCMV strains, either being clinical isolates or laboratory-adapted strains, were able to boost cytokine secretion by Vγ9Vδ2 cells after ABP treatment (Fig. 2A, 2B).

As HCMV can infect multiple cell lineages in vivo, we tested whether infection of other cell types could also stimulate lymphokine production. Infection of primary fibroblasts instead of MRC-5 cells gave identical results (not shown). Vγ9Vδ2 cell stimulation with the astrocytoma U-373MG treated with ZOL induced dose-dependent IFN-γ and TNF secretion in the absence of infection. Nevertheless, infection with either AD169 or VHL/E increased the production of both cytokines (Fig. 2C). To determine whether Vγ9Vδ2 cells were also able to sense HCMV infection in cells of the myeloid lineage, we produced monocyte-derived DCs by in vitro culture of sorted monocytes in the presence of IL-4 and GM-CSF for 5 d. In vitro differentiation of monocytes into DCs was checked by the loss of CD14 expression and upregulation of CD86; VHL/E was used because, unlike AD169, it is known to retain infectivity for myeloid cells. DC permissiveness was checked by the nuclear expression of HCMV-IE protein and was ~3–5% when using an MOI of 5 (Supplemental Fig. 1). After infection with HCMV-VHL/E, DCs were treated with ZOL and cocultured with Vγ9Vδ2 cells. IFN-γ production in the presence of infected DCs was increased compared with cocultures with uninfected DCs. TNF production remained very low even in

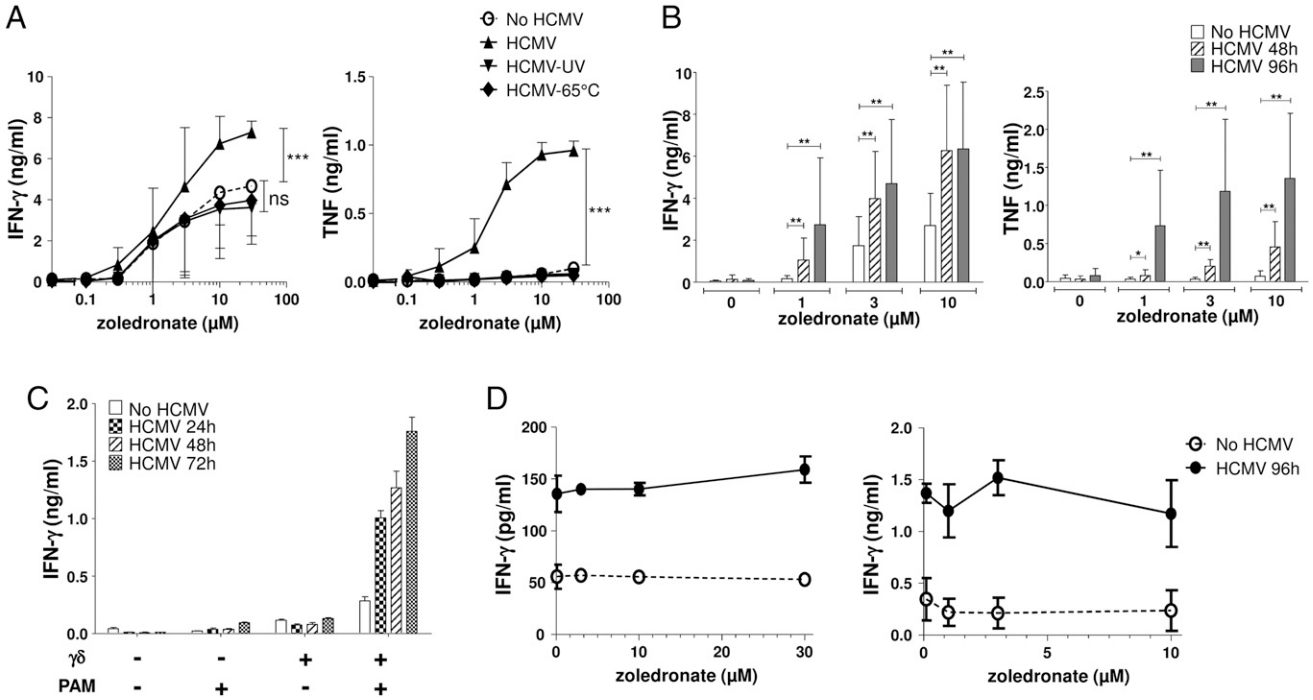

FIGURE 1. Lymphokine secretion by Vγ9Vδ2 cell lines stimulated with HCMV-infected fibroblasts. Vγ9Vδ2 T cell lines were cocultured in microculture wells with MRC-5 fibroblasts (1:1 ratio) that had been infected with HCMV (AD169, MOI of 1) and treated with ABPs. IFN-γ and TNF production were quantified by ELISA after 48 h. (**A**) MRC-5 cells were either mock infected (no virus), infected with untreated HCMV (AD169 strain, MOI of 1), or infected with heat-inactivated (65°C, 30 min) or UV-irradiated virus, during 72 h before coculture. ZOL was added during the last 16 h and washed before addition of γδ cells (means ± SD of four independent triplicate cultures). (**B**) MRC-5 cells were infected or not with AD169 (MOI of 1) 48 or 96 h and treated with ZOL 16 h before coculture with γδ cells; a mean of nine independent experiments were performed in triplicates. (**C**) MRC-5 cells were infected with AD169 during 24, 48, or 72 h and treated or not with pamidronate (PAM, 100 μM) 16 h before coculture with γδ cells or medium only to check for cytokine secretion by fibroblasts (mean of triplicate cultures). (**D**) IFN-γ secretion by HCMV-reactive non-Vδ2 cells in response to MRC-5 cells with or without HCMV infection and ZOL treatment. *Left panel*, $V\delta2^-$ γδ cells (ND2LES). *Right panel*, HLA-A2–restricted, pp65-specific $CD8^+TCR\alpha\beta^+$ clone (CMV-NVL). Error bars indicate SD. $*p < 0.05$, $**p < 0.01$, $***p < 0.001$ [(A) ANCOVA, (B) Wilcoxon test].

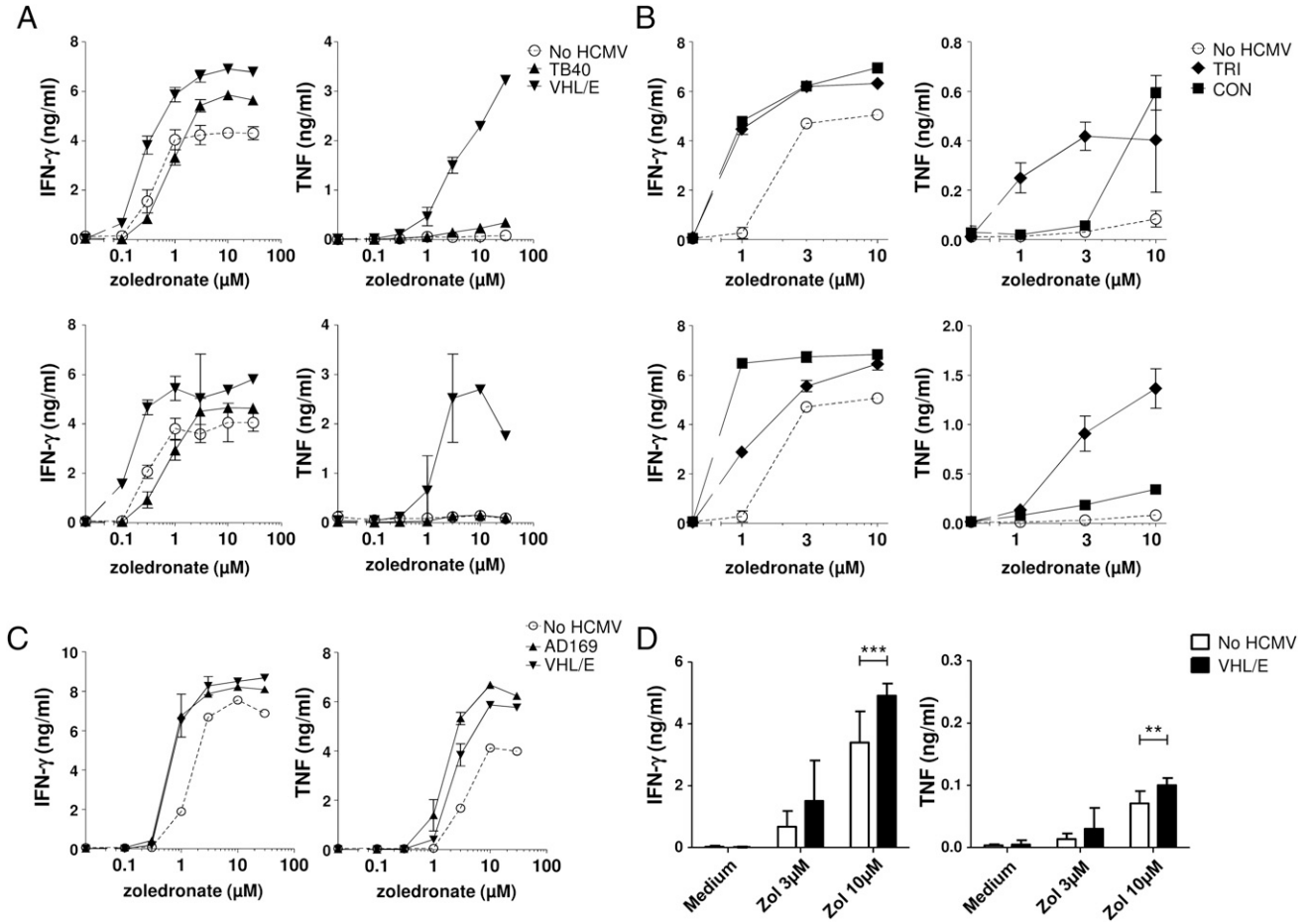

FIGURE 2. Vγ9Vδ2 response to different HCMV strains and nonfibroblast targets. Production of IFN-γ (*left panels*) and TNF (*right panels*) by Vγ9Vδ2 T cells was quantified as in Fig. 1A. (**A** and **B**) Coculture with MRC-5 fibroblasts infected with various HCMV strains (MOI of 1) during 48 (*top panels*) or 96 h (*bottom panels*). TB40/E and VHL/E (A) are laboratory-adapted strains; CON and TRI (B) are low-passage clinical isolates. Each strain was tested at least twice with similar results; one representative experiment is shown (mean ± SD of triplicate cultures). (**C**) Coculture with U-373MG astrocytoma cells infected 48 h with AD169 and VHL/E (MOI of 1); repeated twice with similar results with two different γδ lines. Means ± SD of triplicate cultures from one experiment are shown. (**D**) Coculture with monocyte-derived DCs infected with VHL/E (MOI of 5). DCs were infected at day 5 after differentiation of $CD14^+$ cells in IL-4 and GM-CSF, treated with ZOL at day 6, and cocultured with Vγ9Vδ2 cells from day 7 for 48 h. Means ± SD of four independent experiments (each in triplicate) are shown. $^{**}p < 0.01$, $^{***}p < 0.001$ (Wilcoxon test).

cocultures of γδ cells with infected DCs (Fig. 2D), possibly due to the relatively low percentage of cells expressing viral proteins. Thus, HCMV infection stimulates the lymphokine response of Vγ9Vδ2 cells in most combinations of viral strain and cellular target in the context of ZOL treatment, although these factors influence qualitatively and quantitatively the responses of Vγ9Vδ2 cells.

Response of "fresh" Vγ9Vδ2 cells to HCMV-infected cells

All of the above experiments were performed using activated Vγ9Vδ2 cell lines obtained after their short-term amplification from PBMCs with (*E*)-4-hydroxy-3-methyl-but-2-enyl pyrophosphate phosphoantigen. Because T cells that had not been primed in vitro may behave differently, we evaluated whether Vγ9Vδ2 cells from fresh PBMC samples could also be activated by ZOL-treated fibroblasts and whether HCMV infection also affected their activation. In agreement with other reports (29), the cytokine response of sorted fresh γδ cells was undetectable (not shown), suggesting that they require accessory cells. Thus we cocultured total PBMCs with fibroblasts, infected or not with HCMV AD169 or VHL/E, and measured the specific activation of $V\gamma9^+$ cells by intracellular staining of IFN-γ and TNF (Fig. 3). In independent cultures with six different PBMC samples, the response of $V\gamma9^+$ cells to uninfected, ZOL-treated fibroblasts was barely detected. This response was significantly higher when fibroblasts were infected with HCMV-AD169 or VHL/E, and most activated cells produced IFN-γ and TNF. This cytokine production was essentially confined to $V\gamma9^+$ cells (Fig. 3A). Thus, fresh Vγ9Vδ2 cells also respond by an increased lymphokine production when stimulated with HCMV-infected ZOL-treated fibroblasts.

HCMV infection modulates endogenous production of phosphoantigens

The effect of HCMV infection on the Vγ9Vδ2 T cell response could result from several nonexclusive mechanisms, including induction of ligands for costimulatory molecules such as NKG2D ligands (MHC class I chain–related A/B and UL16-binding proteins proteins), modulation of molecules involved in the sensing of phosphoantigens (such as BTN3A1), or soluble factors. Supernatants from infected cells did not efficiently synergize with ZOL (not shown). The anti-BTN3A1 Ab 103.2 pulsed on targets has been reported to alter the recognition of cells producing phosphoantigens (30). We observed that pulsing this Ab on ZOL-treated cells, infected or not, strongly depressed Vγ9Vδ2 T cell responses whereas responses to CD3 crosslinking were preserved. Blocking the NKG2D activation pathways with an NKG2D-Fc

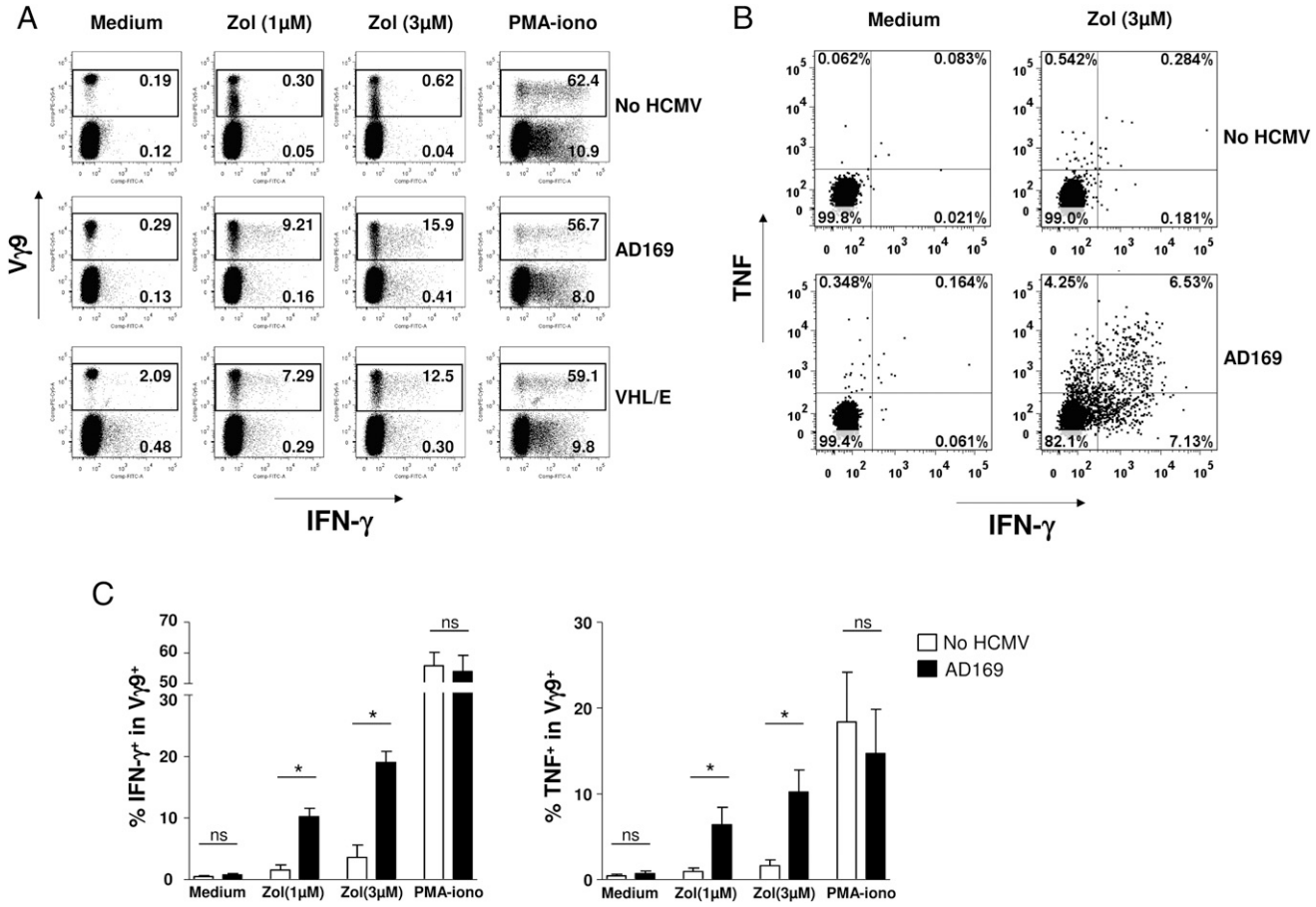

FIGURE 3. FACS analysis of fresh Vγ9$^+$ cell responses to HCMV-infected fibroblasts. MRC-5 fibroblasts were infected by HCMV (AD169 or VHL/E; MOI of 1) for 48 h and treated with ZOL at the indicated concentration during the last 16 h. Fresh unsorted PBMCs were then added for 16 h and brefeldin A was added during the last 4 h of coculture. In some cultures, PMA and ionomycin were added instead of ZOL during 4 h to assess maximal response. Nonadherent cells were then recovered, stained for surface Vγ9 expression and intracellular IFN-γ and TNF accumulation, and analyzed by FACS. (**A** and **B**) Representative dot plots from one individual showing percentages of IFN-γ production in Vγ9$^+$ gate and Vγ9$^-$ cells (A), and double staining for IFN-γ and TNF in Vγ9$^+$ cells (B). (**C**) IFN-γ– and TNF-producing cells in Vγ9$^+$ cells; means ± SD of results from six different healthy donors are shown. *$p <$ 0.05 (Wilcoxon test).

chimera did not significantly affect responses (Supplemental Fig. 2). Although these experiments do not preclude additional effects of ZOL, they suggest an accessory role of cytokines or NKG2D ligands whereas an activation of the TCR/BTN3A1/IPP axis is required.

ABPs inhibit the mevalonate pathway enzyme farnesyl pyrophosphate synthase and promote accumulation of Vγ9Vδ2 T cell agonists such as IPP and ApppI. Nevertheless, they also affect cellular metabolism independently of farnesyl pyrophosphate synthase inhibition (31–33). To check that Vγ9Vδ2 T cell activation by ZOL-treated MRC5 cells, infected or not, was dependent on modulation of the mevalonate pathway, fibroblasts were treated with mevastatin for 24 h prior to addition of ZOL to block the synthesis of mevalonate and downstream metabolites. Mevastatin treatment of fibroblasts abrogated IFN-γ and TNF production by Vγ9Vδ2 cells in a dose-dependent manner (Fig. 4A). Then we measured the intracellular concentration of endogenous phosphoantigens in ZOL-treated fibroblasts, infected or not, using ionic chromatography coupled to tandem mass spectrometry. The limits of detection and of quantification were 0.1 and 0.3 μM (IPP) and 0.01 and 0.03 μM (ApppI), respectively. Note that our procedure does not distinguish IPP and ApppI from their respective isomers DMAPP and ApppD (34). The intracellular amounts of IPP and of its adenylated derivative ApppI (35) were both increased in a dose-dependent manner after ZOL treatment. Importantly, the amount of both metabolites was strongly increased when cells had been infected for 48 h. Intracellular IPP decreased but was still elevated in cells that had been infected for 96 h, whereas ApppI returned below the limit of detection (Fig. 4B). Mevastatin addition prior to ZOL treatment of fibroblasts, infected or not, decreased IPP/ApppI to below the detection level (Fig. 4C). This indicates that HCMV infection boosts the accumulation of endogenous phosphoantigens following ZOL treatment and explains, at least in part, the synergy between ZOL and HCMV for Vγ9Vδ2 stimulation.

HCMV infection affects ZOL capture and mevalonate pathway enzymes

Modulation of the mevalonate pathway has been reported after infection by several viruses, including herpes viruses (36, 37). We thus investigated the effect of HCMV infection on this pathway by measuring the expression of HMG-CoA synthase and HMG-CoA reductase mRNA by quantitative RT-PCR (Fig. 4D). The transcription of both enzymes increased 5- to 10-fold following infection, indicating that this pathway is strongly upregulated in our conditions since the initial phase of infection.

The increased production of phosphoantigens could also possibly result from an increased capture of ZOL by infected cells. To test for this alternative mechanism, we used a fluorescent, CFSE-labeled ZOL derivative, FluorZol (26). The capture of FluorZol by

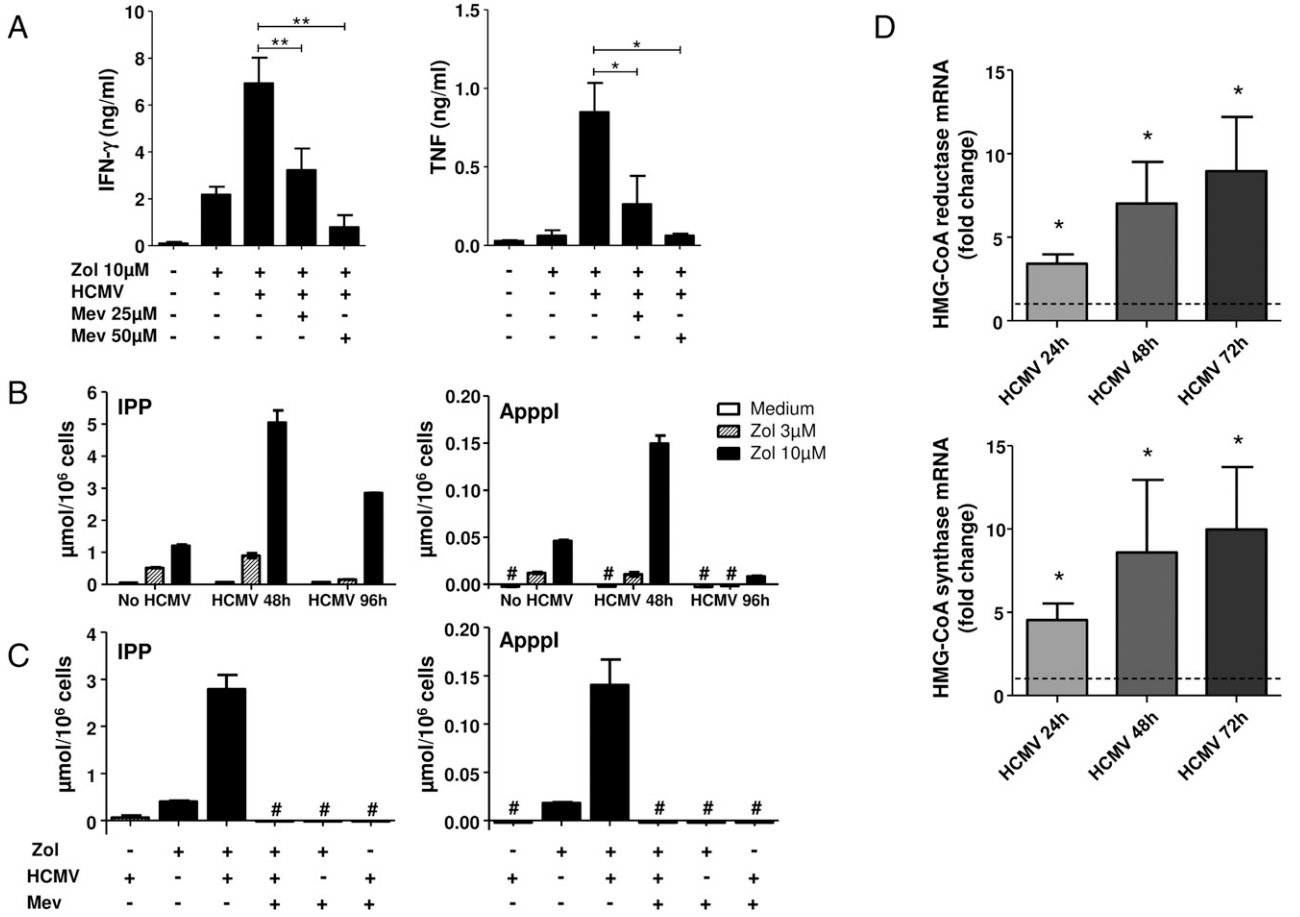

FIGURE 4. Involvement of the mevalonate pathway and phosphoantigen production. (**A**) MRC-5 fibroblasts were infected with HCMV-AD169 (MOI of 1) during 72 h. Vγ9Vδ2 T cells were then added and IFN-γ and TNF production were quantified as in Fig. 1A; in some cultures mevastatin (50 μM, or control solvent) and ZOL (10 μM) were added 40 and 16 h, respectively, before the addition of γδ cells. Means ± SD of three independent experiments in triplicate cultures are shown. (**B** and **C**) IPP and ApppI phosphoantigens were quantified by ion chromatography–coupled tandem mass spectrometry in cytosolic extracts from MRC-5 fibroblasts that had been either not infected or infected with HCMV-AD169 (MOI of 1) during 48 (B and C) or 96 h (C). In some cultures mevastatin (50 μM) and ZOL (10 μM) were added during the last 40 and 16 h, respectively (C). (**D**) MRC-5 fibroblasts were infected with HCMV (AD169; MOI of 1) for 24, 48, or 72 h. HMG-CoA reductase and synthase mRNA expression was measured by quantitative RT-PCR. The results are expressed as the ratio of HMG-CoA reductase and synthase expression in infected cultures over uninfected cultures (fold change, $2^{-\Delta\Delta Ct}$). The dotted lines indicate the reference level (uninfected cells). Means ± SD from six cultures are shown. *$p < 0.05$, **$p < 0.01$, Wilcoxon test. #below limit of detection. Mev, mevastatin.

fibroblasts leads to a dose-dependent increase of fluorescence that can be quantitated by FACS. Moreover, this compound retains the biological activity of ZOL and efficiently synergizes with HCMV infection to stimulate lymphockine secretion by Vγ9Vδ2 cells (Supplemental Fig. 3). Strikingly, the uptake of FluorZol increased gradually in fibroblasts following 24–72 h of infection (Fig. 5). Overall, these experiments indicate that HCMV infection increases the efficiency of ZOL by at least two mechanisms, first by increasing the uptake or retention of ZOL and second by activating the phosphoantigen synthesis pathway.

Vγ9Vδ2 cells can control HCMV replication

The synergistic effect of ZOL and HCMV on cytokine release by Vγ9Vδ2 cells suggests that this drug could be used to specifically target infected cells and possibly limit viral amplification. The coculture conditions used in the above experiments to demonstrate the effect of HCMV on lymphokine secretion resulted in a rapid disruption of the fibroblast layer by Vγ9Vδ2 cell lines even in the absence of infection and were not appropriate for examining viral amplification on a complete viral cycle (5–7 d). To evaluate the antiviral potential of Vγ9Vδ2 cells, we switched to cultures where ZOL was kept at a low concentration all along the coculture with T cells. When the concentration of ZOL was kept at <0.5 μM and the Vγ9Vδ2/fibroblast ratio was ~1:5, uninfected fibroblasts were not altered and the layer was respected. An MOI of ~0.2 was used to allow quantification of the percentage of infected fibroblasts by fluorescence in all conditions. Fibroblasts were thus cultured in medium containing ZOL and subsequently infected with HCMV-AD169. Three hours after infection, a Vγ9Vδ2 cell line was added to the culture for 6 d. The replication cycle of HCMV was followed by monitoring HCMV-IE and HCMV-pp28 protein expression on the fibroblast layer, quantification of HCMV-IE (IE1 plus IE2) mRNA by quantitative RT-PCR in cell lysates, and quantification of infectious particles in supernatants (Fig. 6). In the absence of γδ cells, we observed only a slight decrease of the percentage of HCMV-IE$^+$ cells in cultures containing ZOL up to 0.4 μM, with no significant decrease of viral mRNA expression and only a slight decrease of virion release (~1 log). In cocultures with Vγ9Vδ2 cells, the percentage of HCMV-IE$^+$ cells decreased gradually with increasing concentrations of ZOL to <10% of the control level (Fig. 6A, 6B). Similar results were obtained by monitoring late phase cytoplasmic HCMV-pp28 protein by fluorescence (Supplemental Fig. 4). HCMV-IE mRNA expression was similarly decreased in cultures contraining γδ cells and ZOL (Fig. 6C).

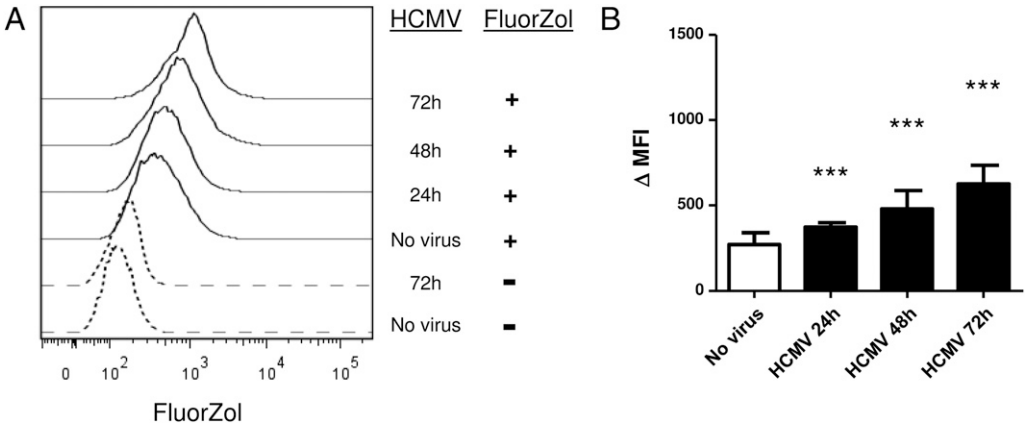

FIGURE 5. ZOL capture by HCMV-infected fibroblasts. MRC-5 fibroblasts were infected by HCMV (AD169, MOI of 1) during the indicated time and pulsed or not with FluorZol (10 μM) during the last 16 h. Fibroblasts were then trypsinized, fixed, and FluorZol internalization was analyzed by FACS. (**A**) Histograms from one representative experiment. (**B**) Cumulative data from four independent experiments. ***$p < 0.001$ (Wilcoxon test). MFI, mean fluorescence intensity; ΔMFI, MFI FluorZol − MFI medium.

The production of infectious virions in the coculture supernatant dropped by approximately three orders of magnitude when Vγ9Vδ2 cells were present and with 0.2–0.4 μM ZOL (Fig. 6D). Thus, Vγ9Vδ2 T cells can potentially limit HCMV replication in presence of submicromolar concentrations of ZOL.

Role of cytokines and cytotoxicity in the control of infection

Activated Vγ9Vδ2 cells are known to develop a potent cytolytic activity in addition to their ability to produce inflammatory cytokines. We wanted to determine which of their activities was determinant for the antiviral effect. We used ^{51}Cr-release assays to examine how HCMV infection affects fibroblast sensitivity to Vγ9Vδ2 killing activity, after ZOL treatment. This could only be evaluated in the initial coculture conditions (Fig. 7A). Vγ9Vδ2 cells displayed a moderate but significant cytolytic activity on ZOL-treated fibroblasts at an E:T ratio of 5:1. This activity was strictly ZOL dose-dependent. HCMV infection of targets did not increase fibroblast lysis. Instead, they became resistant to lysis after 24–48 h of infection. Thus cytolytic activity is unlikely to be responsible for the inhibition of viral replication in cocultures with Vγ9Vδ2 cells.

IFN-γ and TNF produced by CD4$^+$ cells have been shown to affect the replication of HCMV and other viruses (38, 39). To determine whether they were involved in the antiviral effect of Vγ9Vδ2 cells, we used the coculture system described in the previous section and monitored viral replication in the presence or absence of anti–IFN-γ and anti-TNF blocking Abs. Both Abs were able to restore partially viral amplification in cocultures of ZOL-treated fibroblasts, with significant increase of the percentage of cells expressing the IE protein, and a concomitant increase of infectious virions in the culture supernatant (Fig. 7B, 7C). Thus the release of IFN-γ and TNF by Vγ9Vδ2 cells is probably the major mechanism by which Vγ9Vδ2 cells limit viral replication in this system.

Discussion

Activation of γδ T cells during HCMV infection is documented in fetuses and in organ-transplanted patients where it involves minor subsets of Vδ2$^-$ lymphocytes. These cells can detect stress-induced Ags such as endothelial protein C receptor (40), and this recognition involves a specific γδ TCR. At present, it is difficult to target these subsets for immunotherapeutic purposes. Alternatively, Vγ9Vδ2 cells are abundant and prone to immunomanipulation by ABPs or phosphoantigens, but there is no report of an alteration of Vγ9Vδ2 numbers or function in the course of HCMV infection. This goes along with our observations that Vγ9Vδ2 cells do not respond in vitro to HCMV-infected cells and seem to ignore HCMV. However, we show in the present study that HCMV infection induces cellular perturbations that can be sensed by Vγ9Vδ2 cells when an additional TCR stimulus is provided.

In our experiments, fibroblasts that have been treated with ABPs such as pamidronate or ZOL are more potent stimulators of cytokine release by Vγ9Vδ2 T cells when they are infected with HCMV, and this infection increases the effect of ZOL by stimulating the accumulation of endogenous phosphoantigens IPP and ApppI. Except in the particular case of Daudi lymphoma, IPP and derived metabolites (ApppI, DMAPP, ApppD) are usually not detected in cells, and this is because IPP is consumed in downstream metabolic reactions (4, 34, 41). Similarly, we show in the present study that it remains below the level of detection in HCMV-infected cells. Upregulation of phosphoantigens by HCMV is revealed when IPP is not consumed due to inhibition of farnesyl pyrophosphate synthase by ZOL.

Previous studies have shown that HCMV infection activates the transcription factor PPAR-γ (42), a transcription factor that also activates the expression of HMG-CoA synthetase and HMG-CoA reductase, the enzymes that control the initial steps of the mevalonate pathway (43). Upregulation of this pathway is possibly important to increase the availability of metabolites essential for the cycle of several viruses, such as geranyl-geranyl pyrophosphate (36, 37). The effect of HCMV on the endogenous production of phosphoantigens was, however, unpredictable, as HCMV infection may also induce an endogenous type 1 IFN response, which was shown to have an opposite effect on this pathway in a murine system (36). In our model HMG-CoA synthase and reductase are strongly upregulated at the level of transcription in HCMV-infected cells. Thus, blocking the farnesyl pyrophosphate synthase with ABPs results in an increased accumulation of upstream metabolites in infected cells. Nevertheless, this may not be the only mechanism that favors the activity of ZOL during infection. Indeed, intracellular ZOL after cell pulse was significantly increased following infection. This is not unprecedented, as HCMV infection was previously reported to favor uptake/retention of vincristine (44).

Strikingly, the accumulation of IPP/ApppI was high at 48 h of infection and decreased thereafter. It is possible that activation of the type 1 IFN response is responsible for the decrease of IPP/ApppI at

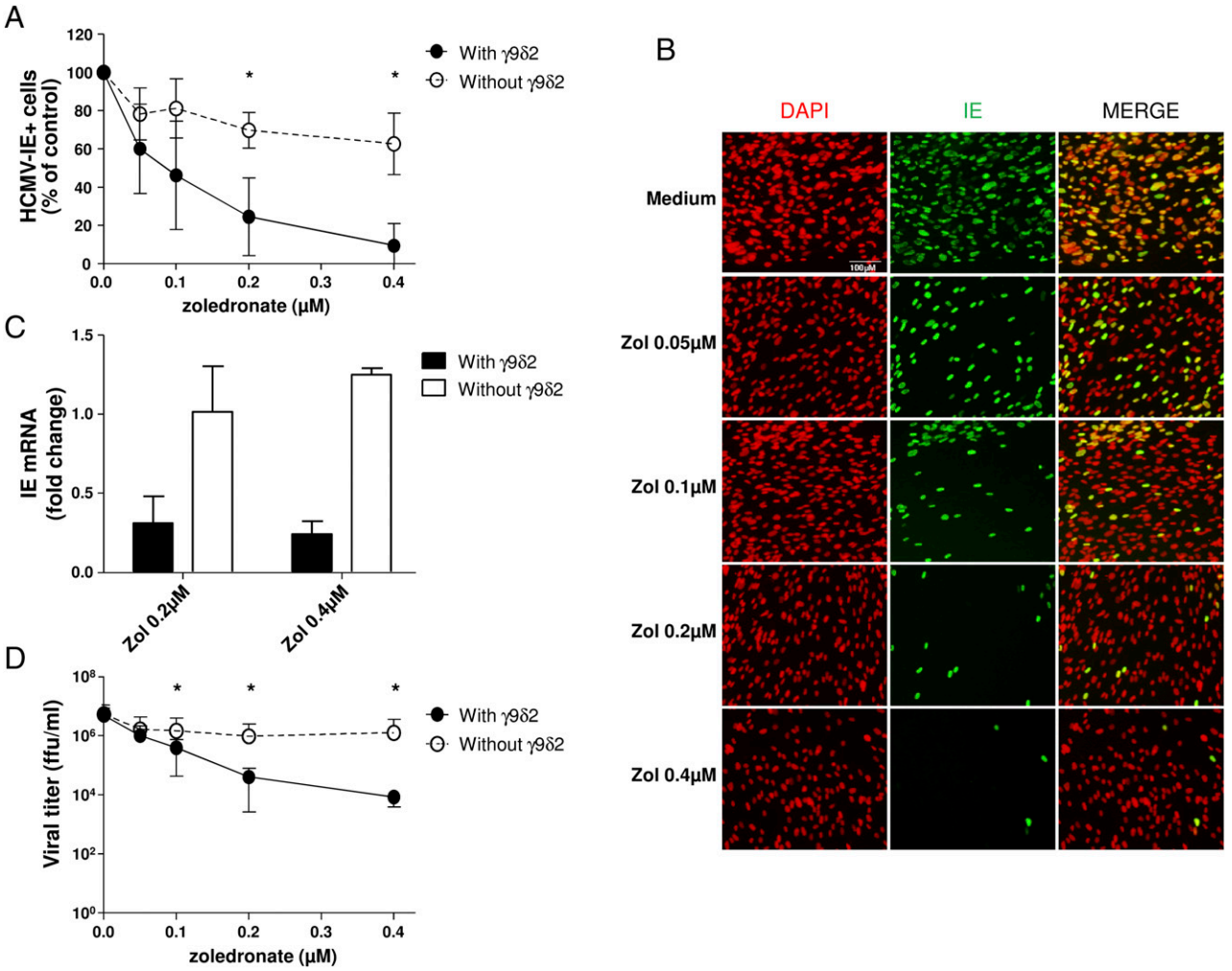

FIGURE 6. Limitation of HCMV replication by Vγ9Vδ2 T cells. (**A** and **B**) MRC-5 cells were cultured in medium containing ZOL at the indicated concentration and infected or not with HCMV (AD169, MOI of 0.2) 3 h before coculture with or without Vγ9Vδ2 cells (T cell line; lymphocyte/fibroblast ratio of 0.2:1). ZOL was maintained in the medium throughout 6 d of coculture. Nonadherent cells were then removed; the adherent fibroblast layer was fixed, stained with anti-IE Abs (FITC, green), and DAPI (red), and analyzed by wide-field fluorescence microscopy for nuclear staining. (A) Cumulative data ($n = 6$) from three independent experiments performed in duplicate cultures (three optic fields, >1500 nuclei for each culture) showing the percentage of infected cells (IE^+ nuclei) among total nuclei ($DAPI^+$). Results are expressed as percentage of the control (without ZOL). (B) Representative images obtained in cocultures of infected fibroblasts with γδ cells, in the absence (medium) or presence of increasing doses of ZOL. Scale bar, 100 μm. (**C**) Cells were cultured as described above. At the end of the 6-d coculture, the fibroblast layer was recovered, total RNA was extracted, and HCMV-IE mRNA expression was measured by quantitative RT-PCR. The results are expressed as the ratio of IE expression in cultures with ZOL over cultures without ZOL (fold change, $2^{-\Delta\Delta Ct}$). Means ± SD of six cultures are shown. (**D**) Infectious HCMV particles in supernatants were titrated at the end of the 6-d coculture by secondary infection of fibroblasts microcultures, immunofluorescence staining with anti-IE Ab, and counting of IE^+ fluorescent focus forming units (ffu). *$p < 0.05$ (Wilcoxon test).

the late phase of infection. However, it is intriguing that the stimulatory activity of infected fibroblasts for lymphokine secretion increases further between 48 and 96 h of infection. It is possible that a transient increase of intracellular phosphoantigens induces long-lasting effects in infected cells, involving, for example, butyrophilin 3A1 rearrangement (30). Nevertheless, additional mechanisms are not excluded and may involve expression of surface molecules or secretion of soluble factors by infected cells.

We show that Vγ9Vδ2 cells have the potential to limit HCMV replication when they are in coculture with infected fibroblasts. Vγ9Vδ2 cells have a potent antitumor activity that is mainly due to their cytolytic potential and is controlled by NKG2D and other NK receptors (45). Our Vγ9Vδ2 cell lines are also cytotoxic in in vitro assays on fibroblasts treated with ZOL at doses >0.4 μM, but, strikingly, infection of fibroblasts with HCMV progressively decreased their sensitivity to lysis during the first 48 h, possibly due to multiple escape mechanisms involving NKG2D ligands. Thus, the main mechanism that allows the control of HCMV amplification in cocultures is probably not a preferential cytolytic activity on HCMV-infected targets. Our results also suggest that escape mechanisms have a distinct impact on cytotoxicity and stimulation of IFN-γ/TNF. HCMV infection may impact the expression of NKG2D ligands in our experiments and leads to resistance to Vγ9Vδ2 cytotoxicity. It has been shown, however, in the case of Vγ9Vδ2 T cells, that NKG2D regulation has little effect on lymphokine secretion (45). Finally, blocking TNF or IFN-γ decreases strongly the antiviral activity of Vγ9Vδ2 T cells, showing that these two cytokines are important antiviral effectors in this system as well as for anti-HCMV CD4 cells (38).

Usage of a synergy between ABPs and HCMV for targeting infected cells with Vγ9Vδ2 T cells requires preservation of non-infected cells; the relative safeness of ABP administration in the clinic even in the presence of IL-2 (46, 47) indicates that this is the case at therapeutic concentrations. However, the peak serum concentration of ZOL after therapeutic intervention is close to or <1 μM (48, 49). As the setting used to demonstrate the

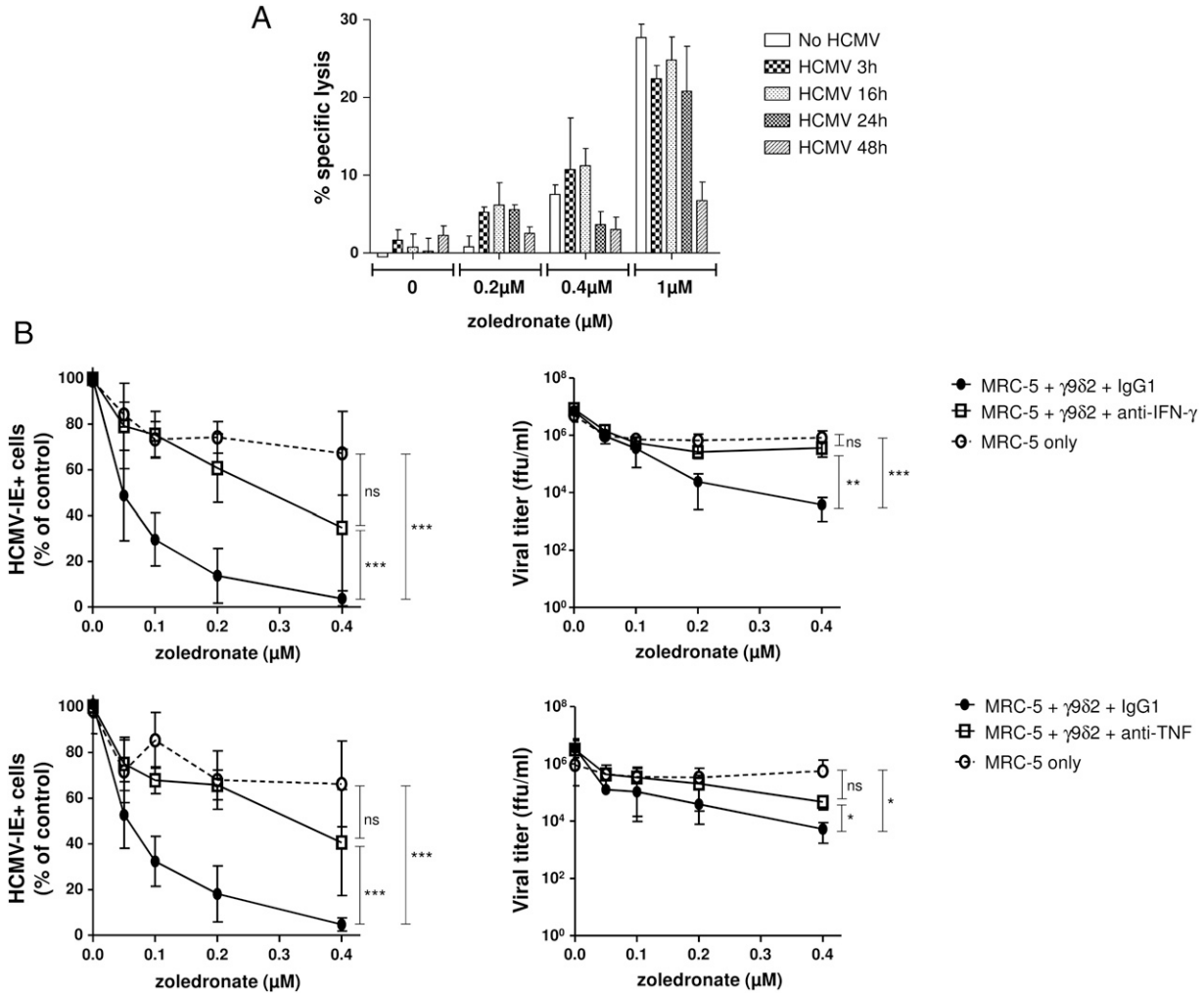

FIGURE 7. Role of cytokines and cytotoxicity in the antiviral effect of Vγ9Vδ2 cells. (**A**) The cytolytic activity of Vγ9Vδ2 cell lines was measured by ^{51}Cr chromium release assays on MRC-5 cells that had been infected (MOI of 1) during 3–48h or not, and treated or not with ZOL for 16 h. A representative experiment out of three with different γδ cell lines is shown. Results are expressed as the mean of specific lysis ± SD of triplicate cultures. (**B**) Cocultures of MRC-5 cells with a Vγ9Vδ2 cell line were performed as described in Fig. 6A and 6B except that anti–IFN-γ (*top panels*), anti-TNF (*bottom panels*), or control Abs were added in the cultures with γδ cells. HCMV-IE expression on the fibroblast layer (*left panels*) and virus release (*right panels*) was measured as in Fig. 6D after 6 d. Results are expressed as the mean ± SD of four cultures from two independent experiments. Covariance analysis was used for the statistical comparison of linearized regression curves. $*p < 0.05$, $**p < 0.01$, $***p < 0.001$.

synergistic effect on lymphokine secretion resulted in unwanted cytotoxicity on noninfected cells, we evaluated an experimental setting where ABPs were maintained at low concentration. ZOL had no detrimental effect on the uninfected cells even in the presence of γδ cells, although it allowed the inhibition of virion release by infected cells by >3 logs in the presence of Vγ9Vδ2 cells. Interestingly, in the absence of γδ cells, the same concentrations produced a slight inhibition of viral replication (~1 log), possibly because optimal viral replication requires downstream mevalonate pathway metabolites (37). Thus, ABPs could be beneficial to control HCMV replication through multiple effects at clinically relevant concentrations.

Based on these in vitro experiments, it will be important to evaluate the effect of ABPs in vivo, in a primate infection model, for example, that would combine permissiveness for HCMV, presence of phosphoantigen-responsive cells, and expression of species-restricted molecules such as BTN3A1. Such a model would allow investigating whether targeting Vγ9Vδ2 T cells with ABPs is useful and safe for controlling infection on the long term or for controlling viral reactivation from latent reservoirs, which is still a challenging issue in the context of transplantation, for example.

Acknowledgments

We are grateful to Franck Halary, Martin Messerle, and Christian Sinzger for providing HCMV strains; to Sabina Muller Valitutti and Vincent Pitard for HCMV-reactive T cell lines; to Emmanuel Scotet for anti-BTN3 Abs; and to Dieter Kabelitz for providing FluorZol. We thank Fatima-Ezzahra L'Faqihi-Olive, Valérie Duplan-Eche, Anne-Laure Iscache (cytometry platform of Centre de Physiopathologie de Toulouse Purpan), Sophie Allard, and Astrid Canivet (imagery platform of Centre de Physiopathologie de Toulouse Purpan) for expert assistance.

Disclosures

The authors have no financial conflicts of interest.

References

1. Eberl, M., M. Hintz, A. Reichenberg, A. K. Kollas, J. Wiesner, and H. Jomaa. 2003. Microbial isoprenoid biosynthesis and human γδ T cell activation. *FEBS Lett.* 544: 4–10.
2. Tanaka, Y., C. T. Morita, Y. Tanaka, E. Nieves, M. B. Brenner, and B. R. Bloom. 1995. Natural and synthetic non-peptide antigens recognized by human γδ T cells. *Nature* 375: 155–158.
3. Thompson, K., J. E. Dunford, F. H. Ebetino, and M. J. Rogers. 2002. Identification of a bisphosphonate that inhibits isopentenyl diphosphate isomerase and farnesyl diphosphate synthase. *Biochem. Biophys. Res. Commun.* 290: 869–873.

4. Gober, H. J., M. Kistowska, L. Angman, P. Jenö, L. Mori, and G. De Libero. 2003. Human T cell receptor γδ cells recognize endogenous mevalonate metabolites in tumor cells. *J. Exp. Med.* 197: 163–168.
5. Kobayashi, H., and Y. Tanaka. 2015. γδ T cell immunotherapy—a review. *Pharmaceuticals (Basel)* 8: 40–61.
6. Poccia, F., C. Gioia, F. Martini, A. Sacchi, P. Piacentini, M. Tempestilli, C. Agrati, A. Amendola, A. Abdeddaim, C. Vlassi, et al. 2009. Zoledronic acid and interleukin-2 treatment improves immunocompetence in HIV-infected persons by activating Vγ9Vδ2 T cells. *AIDS* 23: 555–565.
7. Harly, C., C. M. Peigné, and E. Scotet. 2014. Molecules and mechanisms implicated in the peculiar antigenic activation process of human Vγ9Vδ2 T cells. *Front. Immunol.* 5: 657.
8. Chien, Y. H., C. Meyer, and M. Bonneville. 2014. γδ T cells: first line of defense and beyond. *Annu. Rev. Immunol.* 32: 121–155.
9. Dimova, T., M. Brouwer, F. Gosselin, J. Tassignon, O. Leo, C. Donner, A. Marchant, and D. Vermijlen. 2015. Effector Vγ9Vδ2 T cells dominate the human fetal γδ T-cell repertoire. *Proc. Natl. Acad. Sci. USA* 112: E556–E565.
10. Sandstrom, A., L. Scharf, G. McRae, A. J. Hawk, S. C. Meredith, and E. J. Adams. 2012. γδ T cell receptors recognize the non-classical major histocompatibility complex (MHC) molecule T22 via conserved anchor residues in a MHC peptide-like fashion. *J. Biol. Chem.* 287: 6035–6043.
11. Vavassori, S., A. Kumar, G. S. Wan, G. S. Ramanjaneyulu, M. Cavallari, S. El Daker, T. Beddoe, A. Theodossis, N. K. Williams, E. Gostick, et al. 2013. Butyrophilin 3A1 binds phosphorylated antigens and stimulates human γδ T cells. *Nat. Immunol.* 14: 908–916.
12. Wang, H., O. Henry, M. D. Distefano, Y. C. Wang, J. Räikkönen, J. Mönkkönen, Y. Tanaka, and C. T. Morita. 2013. Butyrophilin 3A1 plays an essential role in prenyl pyrophosphate stimulation of human Vγ2Vδ2 T cells. *J. Immunol.* 191: 1029–1042.
13. Rhodes, D. A., H. C. Chen, A. J. Price, A. H. Keeble, M. S. Davey, L. C. James, M. Eberl, and J. Trowsdale. 2015. Activation of human γδ T cells by cytosolic interactions of BTN3A1 with soluble phosphoantigens and the cytoskeletal adaptor periplakin. *J. Immunol.* 194: 2390–2398.
14. Scotet, E., L. O. Martinez, E. Grant, R. Barbaras, P. Jenö, M. Guiraud, B. Monsarrat, X. Saulquin, S. Maillet, J. P. Estève, et al. 2005. Tumor recognition following Vγ9Vδ2 T cell receptor interactions with a surface F1-ATPase-related structure and apolipoprotein A-I. *Immunity* 22: 71–80.
15. Lafarge, X., P. Merville, M. C. Cazin, F. Bergé, L. Potaux, J. F. Moreau, and J. Déchanet-Merville. 2001. Cytomegalovirus infection in transplant recipients resolves when circulating γδ T lymphocytes expand, suggesting a protective antiviral role. *J. Infect. Dis.* 184: 533–541.
16. Agrati, C., G. D'Offizi, M. L. Gougeon, M. Malkovsky, A. Sacchi, R. Casetti, V. Bordoni, E. Cimini, and F. Martini. 2011. Innate gamma/delta T-cells during HIV infection: terra relatively incognita in novel vaccination strategies? *AIDS Rev.* 13: 3–12.
17. Cummings, J. S., C. Cairo, C. Armstrong, C. E. Davis, and C. D. Pauza. 2008. Impacts of HIV infection on Vγ2Vδ2 T cell phenotype and function: a mechanism for reduced tumor immunity in AIDS. *J. Leukoc. Biol.* 84: 371–379.
18. Cimini, E., C. Bonnafous, V. Bordoni, E. Lalle, H. Sicard, A. Sacchi, G. Berno, C. Gioia, G. D'Offizi, U. Visco Comandini, et al. 2012. Interferon-α improves phosphoantigen-induced Vγ9Vδ2 T-cells interferon-γ production during chronic HCV infection. *PLoS One* 7: e37014.
19. Cimini, E., C. Bonnafous, H. Sicard, C. Vlassi, G. D'Offizi, M. R. Capobianchi, F. Martini, and C. Agrati. 2013. In vivo interferon-α/ribavirin treatment modulates Vγ9Vδ2 T-cell function during chronic HCV infection. *J. Interferon Cytokine Res.* 33: 136–141.
20. Tu, W., J. Zheng, Y. Liu, S. F. Sia, M. Liu, G. Qin, I. H. Ng, Z. Xiang, K. T. Lam, J. S. Peiris, and Y. L. Lau. 2011. The aminobisphosphonate pamidronate controls influenza pathogenesis by expanding a γδ T cell population in humanized mice. *J. Exp. Med.* 208: 1511–1522.
21. Lučin, P., H. Mahmutefendić, G. Blagojević Zagorac, and M. Ilić Tomaš. 2015. Cytomegalovirus immune evasion by perturbation of endosomal trafficking. *Cell. Mol. Immunol.* 12: 154–169.
22. Fielding, C. A., R. Aicheler, R. J. Stanton, E. C. Wang, S. Han, S. Seirafian, J. Davies, B. P. McSharry, M. P. Weekes, P. R. Antrobus, et al. 2014. Two novel human cytomegalovirus NK cell evasion functions target MICA for lysosomal degradation. *PLoS Pathog.* 10: e1004058.
23. Halenius, A., C. Gerke, and H. Hengel. 2015. Classical and non-classical MHC I molecule manipulation by human cytomegalovirus: so many targets—but how many arrows in the quiver? *Cell. Mol. Immunol.* 12: 139–153.
24. Carlier, J., H. Martin, B. Mariamé, B. Rauwel, C. Mengelle, H. Weclawiak, A. Coaquette, C. Vauchy, P. Rohrlich, N. Kamar, et al. 2011. Paracrine inhibition of GM-CSF signaling by human cytomegalovirus in monocytes differentiating to dendritic cells. *Blood* 118: 6783–6792.
25. Wu, L., M. R. Mashego, J. C. van Dam, A. M. Proell, J. L. Vinke, C. Ras, W. A. van Winden, W. M. van Gulik, and J. J. Heijnen. 2005. Quantitative analysis of the microbial metabolome by isotope dilution mass spectrometry using uniformly ^{13}C-labeled cell extracts as internal standards. *Anal. Biochem.* 336: 164–171.
26. Chandrasekaran, V., S. Kalyan, V. Biel, M. Lettau, P. T. Nerdal, H.-H. Oberg, D. Wesch, T. K. Lindhorst, and D. Kabelitz. 2015. Novel synthesis of fluorochrome-coupled zoledronate with preserved functional activity on gamma/delta T cells and tumor cells. *MedChemComm* 6: 919–925.
27. Fortunato, E. A., A. K. McElroy, I. Sanchez, and D. H. Spector. 2000. Exploitation of cellular signaling and regulatory pathways by human cytomegalovirus. *Trends Microbiol.* 8: 111–119.
28. Cha, T. A., E. Tom, G. W. Kemble, G. M. Duke, E. S. Mocarski, and R. R. Spaete. 1996. Human cytomegalovirus clinical isolates carry at least 19 genes not found in laboratory strains. *J. Virol.* 70: 78–83.
29. Miyagawa, F., Y. Tanaka, S. Yamashita, and N. Minato. 2001. Essential requirement of antigen presentation by monocyte lineage cells for the activation of primary human γδ T cells by aminobisphosphonate antigen. *J. Immunol.* 166: 5508–5514.
30. Harly, C., Y. Guillaume, S. Nedellec, C. M. Peigné, H. Mönkkönen, J. Mönkkönen, J. Li, J. Kuball, E. J. Adams, S. Netzer, et al. 2012. Key implication of CD277/butyrophilin-3 (BTN3A) in cellular stress sensing by a major human γδ T-cell subset. *Blood* 120: 2269–2279.
31. Nussbaumer, O., G. Gruenbacher, H. Gander, and M. Thurnher. 2011. DC-like cell-dependent activation of human natural killer cells by the bisphosphonate zoledronic acid is regulated by γδ T lymphocytes. *Blood* 118: 2743–2751.
32. Schmidt, A., S. J. Rutledge, N. Endo, E. E. Opas, H. Tanaka, G. Wesolowski, C. T. Leu, Z. Huang, C. Ramachandaran, S. B. Rodan, and G. A. Rodan. 1996. Protein-tyrosine phosphatase activity regulates osteoclast formation and function: inhibition by alendronate. *Proc. Natl. Acad. Sci. USA* 93: 3068–3073.
33. Skorey, K., H. D. Ly, J. Kelly, M. Hammond, C. Ramachandran, Z. Huang, M. J. Gresser, and Q. Wang. 1997. How does alendronate inhibit protein-tyrosine phosphatases? *J. Biol. Chem.* 272: 22472–22480.
34. Jauhiainen, M., H. Mönkkönen, J. Räikkönen, J. Mönkkönen, and S. Auriola. 2009. Analysis of endogenous ATP analogs and mevalonate pathway metabolites in cancer cell cultures using liquid chromatography-electrospray ionization mass spectrometry. *J. Chromatogr. B Analyt. Technol. Biomed. Life Sci.* 877: 2967–2975.
35. Vantourout, P., and A. Hayday. 2013. Six-of-the-best: unique contributions of γδ T cells to immunology. *Nat. Rev. Immunol.* 13: 88–100.
36. Blanc, M., W. Y. Hsieh, K. A. Robertson, S. Watterson, G. Shui, P. Lacaze, M. Khondoker, P. Dickinson, G. Sing, S. Rodríguez-Martín, et al. 2011. Host defense against viral infection involves interferon mediated down-regulation of sterol biosynthesis. *PLoS Biol.* 9: e1000598.
37. Ye, J., C. Wang, R. Sumpter, Jr., M. S. Brown, J. L. Goldstein, and M. Gale, Jr. 2003. Disruption of hepatitis C virus RNA replication through inhibition of host protein geranylgeranylation. *Proc. Natl. Acad. Sci. USA* 100: 15865–15870.
38. Davignon, J. L., P. Castanié, J. A. Yorke, N. Gautier, D. Clément, and C. Davrinche. 1996. Anti-human cytomegalovirus activity of cytokines produced by CD4$^+$ T-cell clones specifically activated by IE1 peptides in vitro. *J. Virol.* 70: 2162–2169.
39. Romero, R., and J. E. Lavine. 1996. Cytokine inhibition of the hepatitis B virus core promoter. *Hepatology* 23: 17–23.
40. Willcox, C. R., V. Pitard, S. Netzer, L. Couzi, M. Salim, T. Silberzahn, J. F. Moreau, A. C. Hayday, B. E. Willcox, and J. Déchanet-Merville. 2012. Cytomegalovirus and tumor stress surveillance by binding of a human γδ T cell antigen receptor to endothelial protein C receptor. *Nat. Immunol.* 13: 872–879.
41. Vantourout, P., J. Mookerjee-Basu, C. Rolland, F. Pont, H. Martin, C. Davrinche, L. O. Martinez, B. Perret, X. Collet, C. Périgaud, et al. 2009. Specific requirements for Vγ9Vδ2 T cell stimulation by a natural adenylated phosphoantigen. *J. Immunol.* 183: 3848–3857.
42. Rauwel, B., B. Mariamé, H. Martin, R. Nielsen, S. Allart, B. Pipy, S. Mandrup, M. D. Devignes, D. Evain-Brion, T. Fournier, and C. Davrinche. 2010. Activation of peroxisome proliferator-activated receptor γ by human cytomegalovirus for de novo replication impairs migration and invasiveness of cytotrophoblasts from early placentas. *J. Virol.* 84: 2946–2954.
43. Iida, K. T., Y. Kawakami, H. Suzuki, H. Sone, H. Shimano, H. Toyoshima, Y. Okuda, and N. Yamada. 2002. PPARγ ligands, troglitazone and pioglitazone, up-regulate expression of HMG-CoA synthase and HMG-CoA reductase gene in THP-1 macrophages. *FEBS Lett.* 520: 177–181.
44. Weekes, M. P., S. Y. Tan, E. Poole, S. Talbot, R. Antrobus, D. L. Smith, C. Montag, S. P. Gygi, J. H. Sinclair, and P. J. Lehner. 2013. Latency-associated degradation of the MRP1 drug transporter during latent human cytomegalovirus infection. *Science* 340: 199–202.
45. Nedellec, S., C. Sabourin, M. Bonneville, and E. Scotet. 2010. NKG2D costimulates human Vγ9Vδ2 T cell antitumor cytotoxicity through protein kinase Cθ-dependent modulation of early TCR-induced calcium and transduction signals. *J. Immunol.* 185: 55–63.
46. Clézardin, P. 2011. Bisphosphonates' antitumor activity: an unravelled side of a multifaceted drug class. *Bone* 48: 71–79.
47. Fournié, J. J., H. Sicard, M. Poupot, C. Bezombes, A. Blanc, F. Romagné, L. Ysebaert, and G. Laurent. 2013. What lessons can be learned from γδ T cell-based cancer immunotherapy trials? *Cell. Mol. Immunol.* 10: 35–41.
48. Chen, T., J. Berenson, R. Vescio, R. Swift, A. Gilchick, S. Goodin, P. LoRusso, P. Ma, C. Ravera, F. Deckert, et al. 2002. Pharmacokinetics and pharmacodynamics of zoledronic acid in cancer patients with bone metastases. *J. Clin. Pharmacol.* 42: 1228–1236.
49. Belmant, C., D. Decise, and J. J. Fournie. 2006. Phosphoantigens and aminobisphosphonates. New leads targeting γδ T lymphocytes for cancer immunotherapy. *Drug Discov. Today* 3: 17–23.